Available online at www.sciencedirect.com

ScienceDirect

Energy Procedia 90 (2016) 412 – 422

Energy Procedia

5th International Conference on Advances in Energy Research, ICAER 2015, 15-17 December 2015, Mumbai, India

Load Shedding in Deregulation Environment and Impact of Photovoltaic System with SMES

Shailendra Singh[a]*, Deepak Tyagi[b] Ashwani Kumar[b],Saurabh Chanana[b]

[a]*Department of Electrical Engineering, IIT-(BHU),Varanasi India*
[b]*Department of Electrical Engineering, NIT, Kurukshetra, India*

Abstract

With the continuous increase in the load, the frequency of the system goes on decreasing and it reaches to its minimum allowable value after the further increase in load will result in more frequent drop resulting in the need of load shedding. To avoid load shedding and control of the frequency of the systems some approach have discussed here. The paper includes modeling of SMES with solar PV array for frequency control of three areas interconnected thermal system in deregulated environment. A comparative analysis of different load frequency control scheme such as:

i) Using conventional integral controller
ii) Using PID controller,
iii) Using additional sources of energy (PV with SMES) on the basis of load to be shed have been discussed.

The effects of bilateral contracts on the dynamics of a system including three areas, each of which consisting of two GENCOS and two Discos has been discussed. A case study of contract violation of DISCO‘s also being incorporated. For all the three strategies the critical load at which frequency of the areas tries to go below minimum allowable range also has been calculated. With the help of MATLAB software using Simulink, results have been obtained. From the comparison results indicates that on using the third strategy (with additional sources) we are increasing the efficiency of the system. When using system with PID controller and additional sources, frequency of the system doesn’t go below minimum allowable range and there is requirement of load shedding has been eliminated.

Peer-review under responsibility of the organizing committee of ICAER 2015

Keywords: Load shedding; Load frequency control; SMES; Photovoltaic; Deregulation;

* Corresponding author. Tel.: +91-9412482849
E-mail address: ssingh.rs.eee14@itbhu.ac.in

Peer-review under responsibility of the organizing committee of ICAER 2015
doi:10.1016/j.egypro.2016.11.208

Nomenclature	
ΔP_{d1}	Change in the load demand for thermal area 1
ΔP_{d2}	Change in the load demand for thermal area 2,
ΔP_{d3}	Change in the load demand for thermal area 3,
Δf_1	Incremental Frequency of thermal area 1,
Δf_2	Incremental Frequency of thermal area 2,
Δf_3	Incremental Frequency of thermal area 3,
T_{ps1}, T_{ps2}, T_{ps3}	Power system time constant of area 1, area 2 and area 3 respectively,
K_{ps1}, K_{ps2}, K_{ps3}	Power system gains of area 1, area 2 and area 3 respectively,
T_{t1}, T_{t2}, T_{t3}	Turbine time constants of area 1, area 2 and area 3 respectively,
T_{g1}, T_{g2}, T_{g3}	Governor time constants of area 1, area 2 and area 3 respectively,
R_1, R_2	Governor speed regulation parameter of area 1,
R_3, R_4	Governor speed regulation parameter of area 2,
R_5, R_6	Governor speed regulation parameter of area 3,
T_{12}, T_{23}, T_{31}	Synchronizing coefficients of area1, area2 and area3 respectively,
B_1, B_2, B_3	Frequency bias constant of area 1, area 2 and area 3, respectively,
K_{i1}, K_{i2}, K_{i3}	Integral gains of area1, area 2 and area 3, respectively,
K_{p1}, K_{p2}, K_p	Proportional gains of area1, area 2 and area 3, respectively,
Kd1, Kd2, Kd3	Differential gains of area1, area 2 and area 3, respectively

1. Introduction

The electric power industry is moving towards a deregulated framework in which consumers will have an opportunity to make a choice among competing provider of electric energy [1]. Deregulation is the collection of restructured rules and economic incentives that the government set up to control and drives the electric power industry [1-6].Deregulated system consists of generation companies (Gencos), distribution companies (Discos), Genco, Transco, Disco, the ISO as a provider of many ancillary services of a vertically integrated utility will have a different role to play and therefore have to be modeled differently. In the deregulation system, AGC has been identified as an important ancillary service and the ISO has a major responsibility to provide this service for operation. The basic approach to AGC is based on the earlier concept with the addition of new concepts of deregulated electricity markets [2-3].In deregulated electricity markets, a Disco can contract individually with any Genco for power and these transactions are made under the supervision of the ISO. To understand how these contracts are implemented, the Disco participation matrix concept is introduced in [2-3]. The information flow of the contract is superimposed on the traditional AGC system to obtain the response of the AGC with the addition of contracts. If we use some energy storage system or some other source of power supply in addition to the power generated by the system itself then, the need of load shedding can be eliminated [7-10]. Keeping this fact in mind, in this paper study with SMES (superconducting magnetic energy storage device) [15-18] and PV (photovoltaic) array [11-14] has been carried out. As PV array is a non-conventional source of energy and SMES is a storage device, SMES can be charged by PV array whenever, the power requirement in the system is met by other sources and at the time of need, SMES and PV both can supply power to reduce the load curtailment[19]. In this paper, PV-SMES combination is used in an interconnected three area thermal- thermal- thermal system. These additional sources are added in such a manner that they will supply when there is a need (i.e., PV array will supply when the frequency of the system to which PV array is connected, tries to go less than the minimum allowable limit otherwise it will charge SMES). The frequency of the systems can be maintained at 57.6 Hz thus, eliminating the need of load shedding. The results are discussed and developed for getting the best strategy to minimize the load to be shed. The effects of bilateral contracts on the dynamics of a system including three areas, each of which consisting of two Gencos and two Discos has been obtained.

2. Modeling of Systems

In this section, a mathematical model of the system under observation has been derived. An interconnected three area thermal-thermal-thermal system has been taken for study. Three strategies have been developed in this paper as shown below:

- Model of system with conventional integral controller
- Model of system with PID controller
- Model with PV array and SMES

To minimize the frequency deviation corresponding to the same amount of load disturbance after finding the transfer function of the system between changes in frequency to change in load disturbance. The time at which frequency deviation is maximum, is found out by using maxima-minima concept and then the maximum deviation in frequency can be found out. According to the deviation in the frequency amount of load to be shed is now can be calculated.

2.1. Model of system with conventional integral controller:

In this model, a block diagram of three areas interconnected thermal-thermal-thermal system with the conventional integral controller used for controlling ACE is shown in Fig. 1. The transfer function of this system is given by:

$$\frac{\Delta F_1(s)}{\Delta P_{d1}(s)} = \frac{N}{D} \tag{1}$$

Where,

$N = 0.0001s^{13} + 0.0006s^{12} + 0.0047s^{11} + 0.0286s^{10} + 0.1329s^9 + 0.4744s^8 + 1.2895s^7 + 2.5881s^6 + 3.6748s^5 + 3.3759s^4 + 1.8908s^3 + 0.5830s^2 + 0.0914s$

$D = 0.002s^{14} + 0.012s^{13} + 0.070s^{12} + 0.322s^{11} + 1.227s^{10} + 3.843s^9 + 9.784s^8 + 19.846s^7 + 30.925s^6 + 34.540s^5 + 25.502s^4 + 12.558s^3 + 4.003s^2 + 0.772s + 0.070$

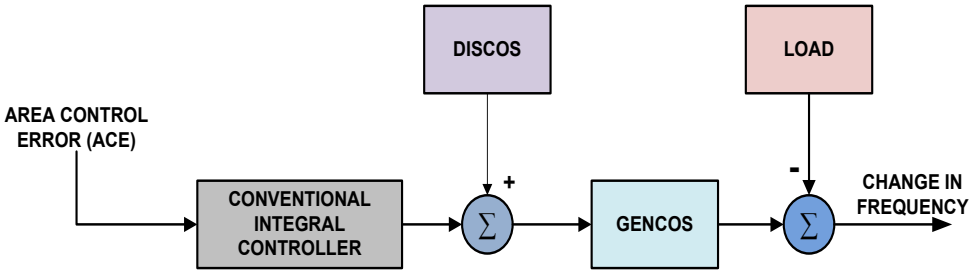

Fig.1. System with conventional integral controller

2.2. Model of system with PID controller:

In this model, PID Controller is used for minimizing the frequency deviation corresponding to load disturbances. PID controller is taking an ACE as its input. The impact of using this in the system is examined by using simulation. The corresponding system is shown in Fig. 2.The transfer function of this system is given by:

$$\frac{\Delta F_1(s)}{\Delta P_{d1}(s)} = \frac{N}{D} \tag{2}$$

Where,

$N = 0.0001s^{13} + 0.0006s^{12} + 0.0047s^{11} + 0.0286s^{10} + 0.1330s^9 + 0.4747s^8 + 1.2905s^7 + 2.5904s^6 + 3.6514s^5 + 3.3791s^4 + 1.8923s^3 + 0.5933s^2 + 0.0914s$

$D = 0.002s^{14} + 0.012s^{13} + 0.070s^{12} + 0.323s^{11} + 1.228s^{10} + 3.846s^9 + 9.792s^8 + 19.866s^7 + 30.959s^6 + 34.580s^5 + 25.531s^4 + 12.570s^3 + 4.006s^2 + 0.773s + 0.070$

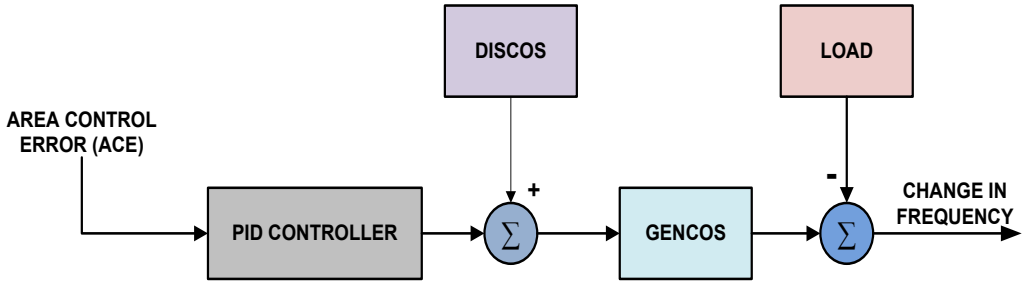

Fig.2. System with PID Controller

2.3. Model with PV array and SMES:

Modelling of photovoltaic and SMES has been discussed in section2.3.1 and 2.3.2 respectively. In this system, PV array has been connected to area1 and area 2 while SMES which is being charged by PV array during low-load condition is connected in area 3. These additional sources start supplying power when the frequency of the corresponding system decrease and tries to go below the minimum allowable frequency limit of 57.6 Hz. For an instant lets temperature is 300C, so power generation will be constant. The transfer function of this system is given by:

$$\frac{\Delta F_1(s)}{\Delta P_{d1}(s)} = \frac{N}{D} \tag{3}$$

Where,

$N = 0.0001s^{14} + 0.0007s^{13} + 0.0044s^{12} + 0.0230s^{11} + 0.0985s^{10} + 0.2906s^{9} + 0.7011s^{8} + 1.2611s^{7} + 1.6201s^{6} + 1.4074s^{5} + 0.7750s^{4} + 0.2545s^{3} + 0.0454s^{2} + 0.0023s$

$D = 0.002s^{15} + 0.011s^{14} + 0.056s^{13} + 0.232s^{12} + 0.802s^{11} + 2.292s^{10} + 5.347s^{9} + 9.964s^{8} + 14.277s^{7} + 14.858s^{6} + 10.637s^{5} + 5.232s^{4} + 1.729s^{3} + 0.365s^{2} + 0.043s + 0.002$

2.3.1. Solar Photovoltaic (PV) system

The PV system is the assembly of PV arrays, connections, protective parts and supports. Arrays are the combination of solar cells. The equivalent circuit of a solar cell is the combination of a current source in parallel with a diode. The output of the current source is directly proportional to the light falling on the cell. Equation of ideal solar cell [13], [17] that represents the ideal solar cell model is:

$$I = I_L - I_R\left[\exp\left(\frac{V}{AV_i}\right) - 1\right] \tag{4}$$

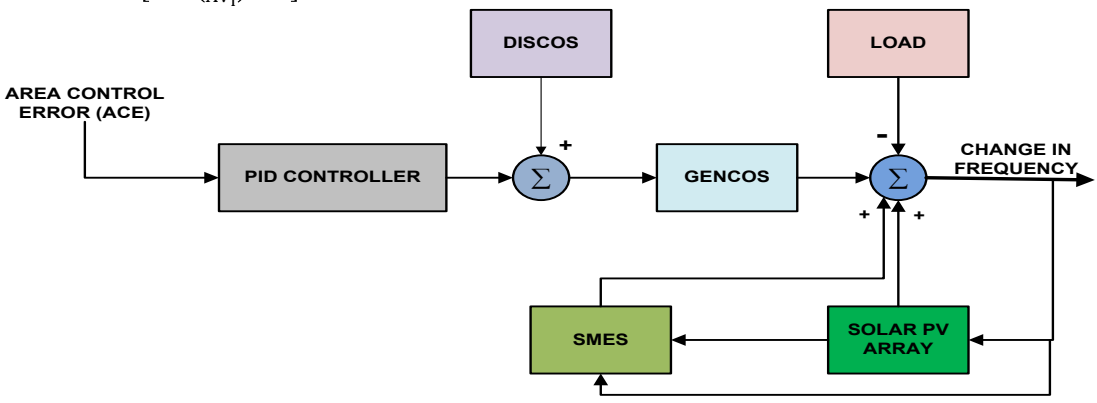

Fig.3. System with PID-LFC using solar PV array and SMES

where:
"I_L" is photocurrent (A); "I_R" is reverse saturation current (A);
"V"is diode voltage (V); " V_i " is thermal voltage, "A" is diode ideality factor.
The photocurrent (I_L) in equation (5) depends on solar irradiance intensity and temperature that is described as:

$$I_L = \frac{\lambda}{\lambda_{ref}} \left[I_{sc,ref} + \mu_{Isc} (T - T_{ref}) \right] \quad (5)$$

where:"$I_{sc,ref}$" is solar cell short –circuit current at reference condition "μ_{Isc}" is the solar cell short-circuit temperature coefficient.
On the other hand, the cell's reverse saturation current is described as:

$$I_R = I_{R,ref} \left(\frac{T}{T_{ref}} \right)^{\frac{3}{A}} \exp \left[qE_g \left(1/T_{ref} - 1/T \right) /kA \right] \quad (6)$$

$$I_{R,ref} = I_{sc,ref} / \left[\exp \left(V_{oc,ref}/AV_i \right) - 1 \right] \quad (7)$$

Where: "$V_{oc,ref}$" is solar cell open circuit voltage at reference condition; " E_g" is a band-gap energy in the solar cell, (1.12-1.15eV).Modified voltage-current characteristic equation of solar cell is given as:

$$I = I_L - I_R \left[\exp \left(\frac{V+IR_{Se}}{AV_i} \right) - 1 \right] - \frac{V+IR_{Se}}{R_{Sh}} \quad (8)$$

A solar PV module is the shape of an assembly of solar cells in series and parallel combination, with their protection device. Current-voltage characteristic equation of equivalent circuit for a PV module arranged in series N_s and parallel N_p can be described as [3]:

$$I^M = N_p I_L - N_p I_R \left[\exp \left(\frac{V^M/N_s + I^M/N_s}{AV_i} \right) \right] - \frac{(N_p/N_s)V^M + I^M R_{Se}}{R_{Sh}} \quad (9)$$

" N_p" is cells parallel number; " N_s " is cells series number
The SESG-ND-216u1F PV module is taken for example, which provides .21 p.u maximum power, and has series connected polycrystalline silicon cells. The key specifications are in Table 1. The model is evaluated-using Matlab/Simulink. The parameters are evaluated during execution using the equations (4-9) listed in the previous section using the data points from Table 1. Detail modelling of PV array has been discussed in previous research work referred to [17].

2.3.2. Configuration of the SMES in the Power System

In the SMES unit, a dc magnetic coil is connected to the ac grid through a Power Conversion System (PCS) which includes an inverter/rectifier. The superconducting coil is contained in a helium vessel. Heat generated is removed by means of a low-temperature refrigerator [19]. Helium is used as the working fluid in the refrigerator as it is the only substance that can exist as either a liquid or a gas at the operating temperature which is near absolute zero. The current in the superconducting coil will be tens of thousands or hundreds of thousands of amperes. No ac power system normally operates at these current levels and hence a transformer is mounted on each side of the converter unit to convert the high voltage and low current of the ac system to the low voltage and high current required by the coil. The energy exchange between the superconducting coil and the electric power system is controlled by a line commutated converter [16], [19]. To reduce the harmonics produced on the ac bus and in the output voltage to the coil, a multi pulse converter or high quality power condition system is preferred. In this study a 12 pulse converter has been considered for the operation of the system [20], [21]. The superconducting coil can be charged to a set value from the grid during normal operation of the power system. Once the superconducting coil gets charged, it conducts current with virtually no losses as the coil is maintained at extremely low temperatures. When there is a sudden rise in the load demand, the stored energy is almost released through the PCS to the power system as alternating current. As the governor and other control mechanisms start working to set the power system to the new equilibrium condition, the coil current changes back to its initial value. The control of the converter firing angle α provides the dc voltage appearing across the inductor to be continuously varying within a certain range of positive and negative values. The inductor is initially charged to its rated current I_{d0} by applying a small positive voltage. Once the current reaches its rated value, it is maintained constant by reducing the voltage across the inductor to zero since the coil is superconducting. Neglecting the transformer and the converter losses, the dc voltage is given

by [16]:

$$Ed = 2V_d\cos\alpha - 2I_dRC. \quad (10)$$

Where Ed is the dc voltage applied to the inductor in kV, α is the firing angle in degrees, I_d is the current flowing through the inductor in kA, RC is the equivalent commutating resistance in kΩ and V_{d0} is the maximum circuit bridge voltage in kV. Charging and discharging of the SMES unit is controlled through the change of commutation angle α. If α is less than 90°, converter acts in the converter mode (charging mode) and if α is greater than 90°, the converter acts in the inverter mode (discharging mode)[16].

2.3.2.1. Control Unit of SMES:

When power is to be pumped back into the grid in the case of a fall in frequency due to sudden loading in the area, the control voltage E_d is to be negative since the current through the inductor and the thyristors cannot change its direction. The incremental change in the voltage applied to the inductor is expressed as:

$$\Delta E_d = \left[\frac{K_{SMES}}{1+sT_{dc}}\right] \Delta Error1 \quad (11)$$

where, ΔE_d is the incremental change in converter voltage; TDC is the converter time delay; K_{SMES} is the gain of the control loop and ΔError is the input signal to the SMES control logic. The inductor current deviation is given by:

$$\Delta I_d = \frac{\Delta E_d}{sL} \quad (12)$$

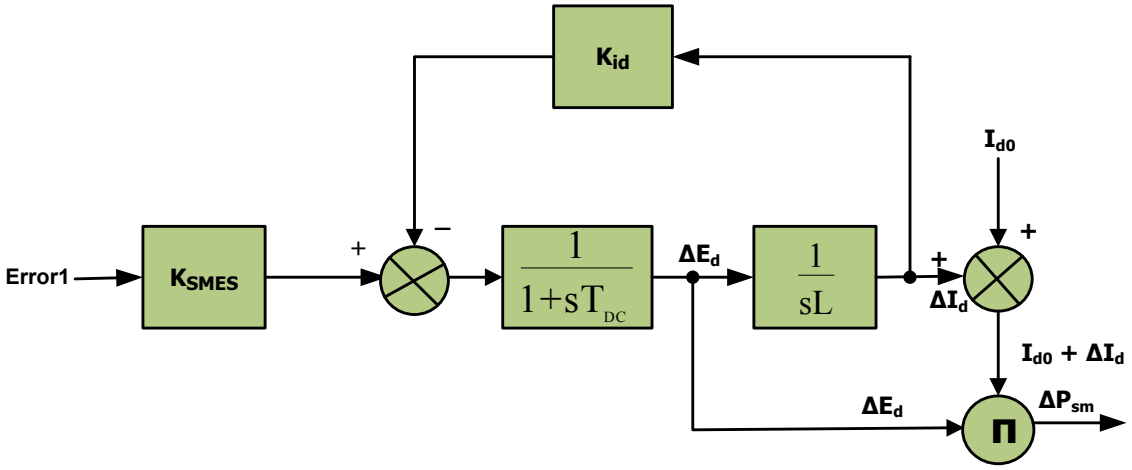

Fig. 4. SMES block diagram with negative inductor current deviation feedback [21]

Here, area control error (ACE) of area 1 is considered as the input signal to the SMES control logic (i.e., ΔError1 = ACE1).

The area control error of the two areas is defined as:

$$ACE_i = B_i\Delta f_i + \Delta P_{tieij}, \qquad i,j=1,2 \quad (13)$$

Where Δfi is the change in frequency of the area i and ΔPij is the change in tie-line power flow out of area i–j. Thus, from above eqs:

$$\Delta E_d = \frac{K_{SMES}}{1+sT_{dc}} (B_1\Delta f_1 + \Delta P_{tie12}) \quad (14)$$

The inductor current in the SMES unit will return to its nominal value very slowly only if Eq. (13) is used. But, the

inductor current must be restored to its nominal value quickly after a system disturbance so that it can respond to the next load perturbation immediately. Hence, the inductor current deviation can be sensed and used as a negative feedback signal in the SMES control loop so that the current restoration to its nominal value can be enhanced.
Thus the dynamic equations for the inductor voltage deviation and the current deviation of the SMES unit area are:

$$\Delta E_d = \frac{[K_{SMES}(B1\Delta f1+\Delta Ptie12)-K_{id}\Delta I_d]}{1+sT_{dc}} \quad (15)$$

Values of parameters used in SMES model have been described at Appendix B.

3. Results and Discussion

This section discussed the analysis of obtained results from Modelling of systems. Models are developed in Matlab / Simulink environment. A case of contract violation is also discussed in this section. DISCO violates a contract by demanding more than that specified in the contract. For obtaining a situation where frequency goes below 57.6 Hz and to show elimination of the need of load shedding 1.5 p.u. excess load demand is taken in all three areas. Due to large mismatch between demand and generation, so there is need of load shedding is required.
Total local load in area 1 = Total local load in area 2 = Total local load in area 3 = 2.0 p.u.
The results obtained for frequency deviations, tie line power deviations, and Gencos power, are shown in Figs 5-16. Figs. 5-7 show the frequency response of the three areas corresponding to load disturbance of 2.0 p.u in all the three areas. Figs. 8-10 show tie line power response of the three areas corresponding to load disturbance of 2.0 p.u in all the three area.

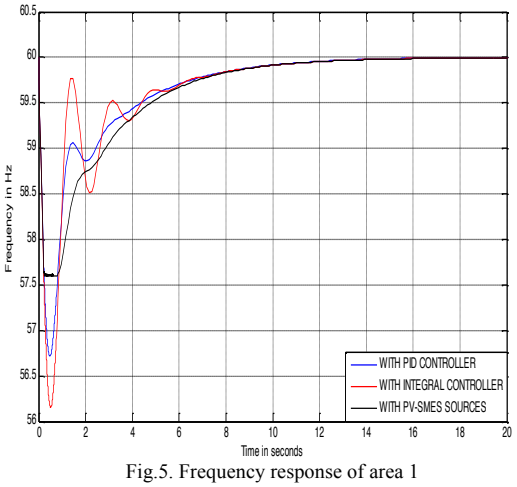

Fig.5. Frequency response of area 1

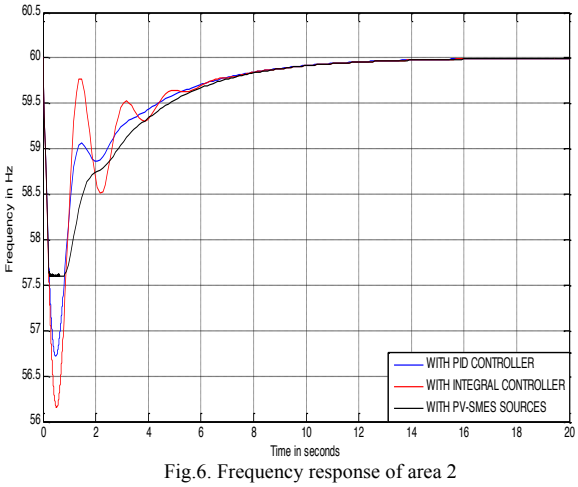

Fig.6. Frequency response of area 2

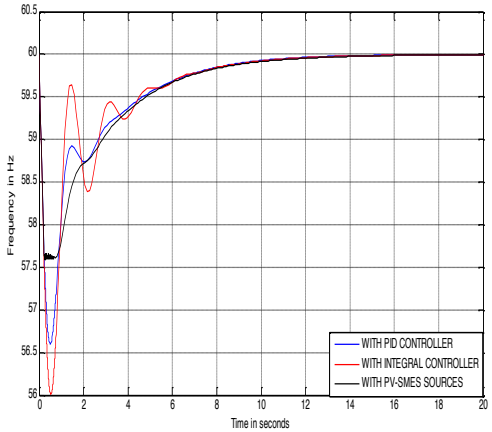

Fig.7. Frequency response of area 3

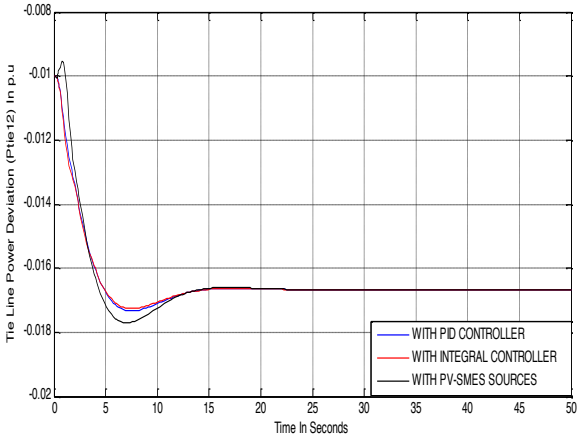

Fig. 8. Variation in tie line power P_{tie12}

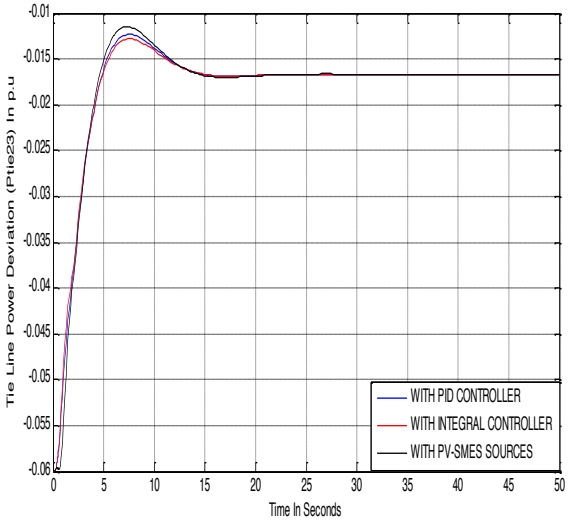

Fig. 9.Variation in tie line power P_{tie23}

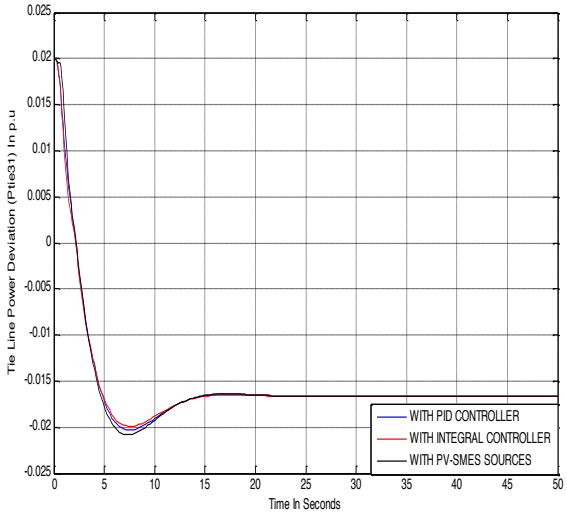

Fig.10. Variation in tie line power Ptie31

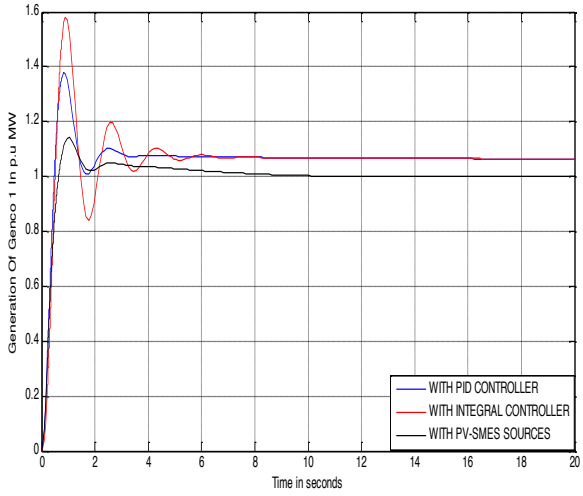

Fig.11. Variation in power generated by Genco 1

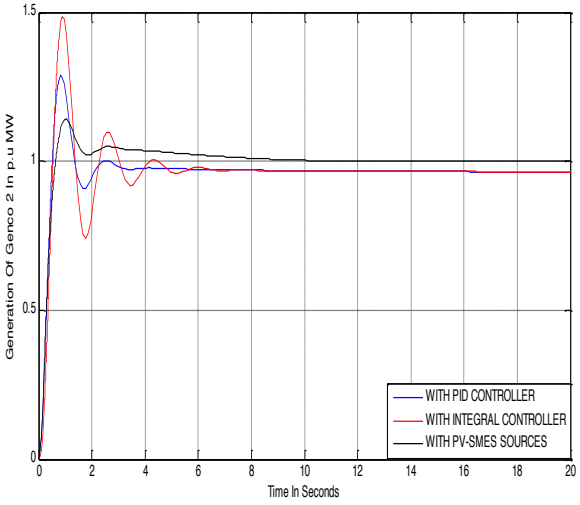

Fig.12. Variation in power generated by Genco2

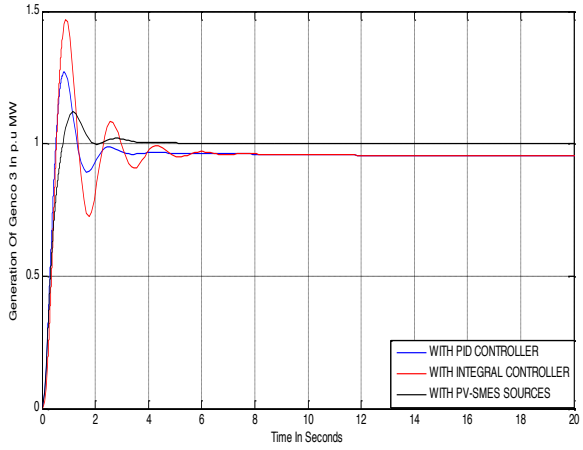

Fig. 13. Variation in power generated by Genco 3

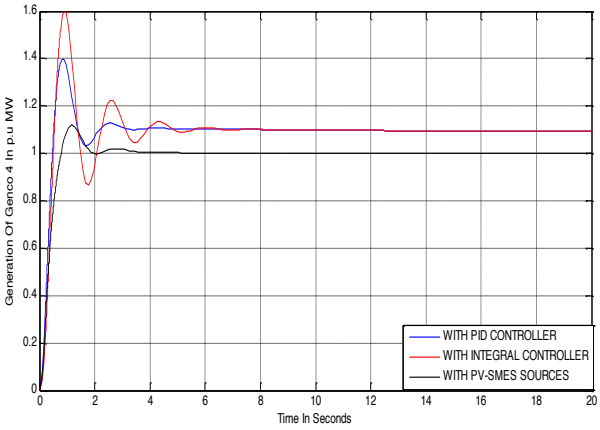

Fig. 14. Variation in power generated by Genco 4

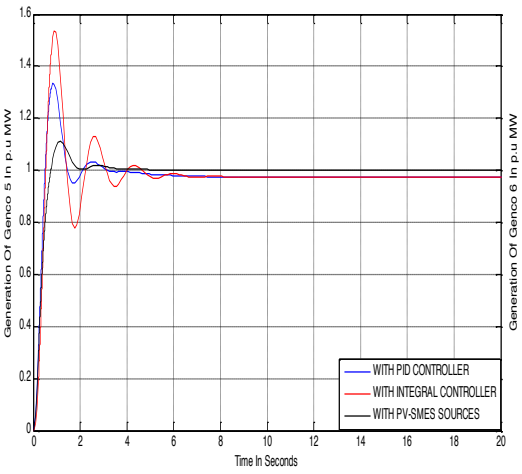

Fig.15. Variation in power generated by Genco 5

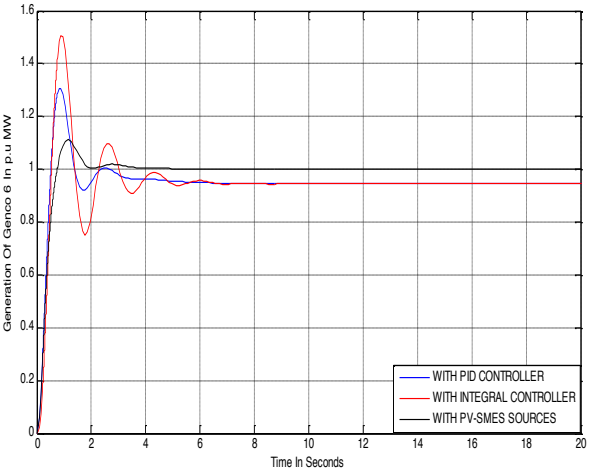

Fig.16. Variation in power generated by Genco 6

Figs. 11-16 show generation response of Gencos connected in all three areas corresponding to load disturbance of 2.0 p.u. From above Figs. 5-16 we can see that in the third strategy (using additional sources of energy), waveforms obtained are best. Also, when due to excess load, frequency of area 1, 2 and area 3 tries to go below 57.6 Hz additional sources supply additional power to maintain frequency within its minimum allowable limit of 57.6 Hz. In the above Figs. 5-16 a comparison between the three strategies discussed has been given. From the comparison it can be conclude that on using third strategy (with additional sources), the efficiency of the system is increased. This can be evidently understood from the above Figs.

With the help of MATLAB, using Simulink we can find out the critical load at which frequency of the areas tries to go below 57.6 Hz for all the three strategies discussed above.

- When using conventional integral controller, for equal load disturbance of 2.0p.u in all areas, we get,
  - For area 1 critical load is 1.288 p.u amount of load to be shed is 0.712 p.u.
  - For area 2 critical load is 1.295 p.u amount of load to be shed is 0.705 p.u.
  - For area 3 critical load is 1.225 p.u amount of load to be shed is 0.775 p.u.
- When using PID controller, for equal load disturbance of 2.0 p.u in all areas, we get,
  - For area 1 critical load is 1.5 p.u amount of load to be shed is 0.5 p.u.
  - For area 2 critical load is 1.51 p.u amount of load to be shed is 0.49 p.u.
  - For area 3 critical load is 1.433 p.u amount of load to be shed is 0.567 p.u.

When using system with PID controller and additional sources like PV array and SMES frequency of the system doesn't go below57.6 Hz, because whenever system frequency tries to go below 57.6 Hz additional sources gives additional power to the system which stops further declination in frequency. Solar system is supplying 0.2 p.u powers for maintaining frequency up to 57.6 Hz. From this strategy deviation in frequency is not more than -2.4 Hz so a requirement of load shedding is eliminated.

4. Comparison of the Strategies:

Comparisons of the given strategies named as 1) Using conventional integral controller, 2) Using PID controller, 3) Using additional sources of energy on the basis of load to be shed.

On using PID controller behaviour of waveforms are improved as there deviation becomes less and there settling time decreases in comparison of system with conventional integral controller.

By using second strategy load to be shed is minimized in each area by amount:

- Saved amount of load in area 1 is 0.512 p.u.
- Saved amount of load in area 2 is 0.515 p.u.
- Saved amount of load in area 3 is 0.508 p.u.

By using third strategy load shedding is eliminated Figs. 5-8. From below Fig. 18 Graph showing minimum frequency of area 1 for different cases it can be seen that for different loads the minimum frequency in first two systems is less than 57.6 Hz while in third system the frequency is at its critical value (57.6 Hz) for same value of load disturbances. Similar graphs can be obtained for remaining two areas also. Thus, eliminating need of Load Shedding.

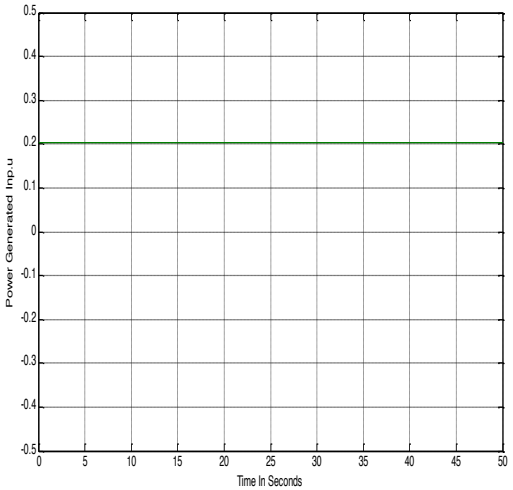

Fig. 17 Waveform of power generated by solar PV array

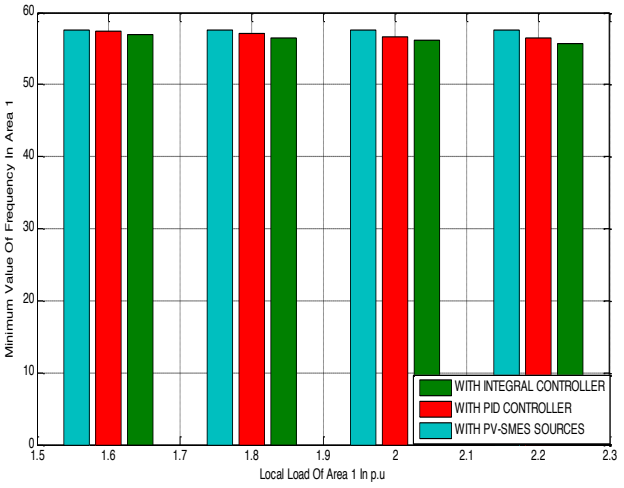

Fig. 18 Graph showing minimum frequency of area 1 for different cases

Table 1 Parameters of PV module

Solar Cell	Poly-crystalline silicon.
Rated output power	203 KW (+10% / -5%)
Open circuit Voltage Voc,ref	30V
Short circuit Current Isc,ref	8.10A
Shunt Resistance RSh	50 ohm
Series Resistance RSe	5 mohm
Diode Ideality factor	1.45
Inverse diode saturation current IR	3.047e-7 A
S.C current temperature coefficient,μIsc	1.73e-3 A / oK
Reference Temperature Tref	30^0C
Dimensions	164cm* 99.40 cm * 4.6 cm

5. Conclusion

In this paper, issue of maintaining frequency in deregulated power system has been presented. The model of power system in deregulated regime of power system using different controllers has been explained. In this paper three different strategies have been developed 1) using conventional integral controller, 2) using PID controller, 3) using non-conventional sources of energy are applied on the three cases of contracts violation.

Tie line power deviations are almost zero and settling time of waveforms decreases on using PID controller. On using these sources, the frequency deviation below 57.6 Hz has been avoided which in turn, eliminates need of load shedding because our under-frequency load shedding scheme applied to those loads for which frequency goes below 57.6 Hz.

Appendix A.

System Data

Kps1 = Kps2 = Kps3 =120 Hz/p.u. MW

Tg1 = Tg2 = Tg3 =0.08 s

R1 = R2 = R3 = R4 = R5 = R6 =3 Hz/p.u. MW
B1 = B2 = B2 = 0.4249
Tt1 = Tt2= Tt3=0.3
Tps1 = Tps2 = Tps3 =20 sec
Ki1= Ki2= Ki3=0.06
Ki=0.6
Kp=0.001
Kd=0.15
$2\Pi T_{12} = 0.0866$
$a_{12} = a_{23} = a_{31} = -1.0$

Appendix B.

SMES Data
L = 2.65 H.
T_{DC} = 0.03 s.
K_{SMES} = 100 kV/unit MW.
K_{id} = 0.2 kV/kA.
I_{d0} = 4.5kA.

References

[1] Maliszewski RM, Dunlop RD, Wilson GL. Frequency actuated load shedding and restoration Part I—philosophy. IEEE Transactions on Power Apparatus and Systems 1971; PAS-90:1452–1459.
[2] Horowitz SH, Polities A, "Gabrielle AF. Frequency actuated load shedding and restoration Part II—implementation." IEEE Transactions on Power Apparatus and Systems1971; PAS-90:1460–1468.
[3] Anderson PM, Mirheydar M. A low-order system frequency response model. IEEE Transactions on Power Systems 1990; 5:720 –729.
[4] Anderson PM, Mirheydar M. An adaptive method for setting under frequency load shedding relays. IEEE Transactions on Power Systems 1990; 7: 647–655.
[5] Lokay HE, Burtnyk V. Application of under-frequency relays for automatic load shedding. IEEE Transactions on Power Apparatus and Systems 1968; PAS-87(5):1362–1366.
[6] Chuvychin VN, Gurov NS, Venkata SS, Brown RE. An adaptive approach to load shedding and spinning reserve control during under-frequency conditions. IEEE Transactions on Power Systems1996; 11:1805–1810.
[7] Qiu B, Liu Y, Chan EK, Cao LL. LAN-based load shedding controller (LSC) for the oil refinery facility. Proceedings of the IEEE Power Engineering Society Winter Meeting 2001; 2: 835–840.
[8] Zhao Q, Chen C. Study on a system frequency response model for a large industrial area load shedding. Electrical Power and Energy System 2005; 27: 233–7.
[9] Bhatt P, Roy R, Ghoshal SP. Optimized multi area AGC simulation in restructured power systems. Electrical Power and Energy System 2010; 32: 311-322.
[10] Donde V, Pai MA, Hiskens I.A. Simulation and optimization in an AGC system after deregulation. IEEE Transactions on Power Systems 2001; 16: 481–489.
[11] Gow JA, Manning CD. Development of a photovoltaic array model for use in power electronics simulation studies. IEE Proceedings on Electric Power Applications 199; 146: 193-200.
[12] Asano H, Yajima K, Kaya A. Influence of photovoltaic power generation of required capacity for load frequency control. IEEE Transactions on Energy Conversion 1996; 11:188-193.
[13] Yanagawa S, Kato T, Wu K, Tabata A, Suzuoki Y. Evaluation of LFC capacity for output fluctuation of photovoltaic generation systems based on multi-point observation of insolation. Proceedings of IEEE PES SM, Vancouver 2001:1652-57.
[14] Chen Qi, Zhu Ming, "Photovoltaic Module Simulink Model for a Stand-alone PV System." Physics Procedia 24 (2012): 94-100.
[15] Abraham RJ, Das D, Patra A, Automatic generation control of an interconnected hydrothermal power system considering smes. Electrical Power and Energy Systems 2007; 27: 571–579.
[16] Banerjee S, Chatergee JK, Tripathy SC. Application of magnetic energy storage unit as continuous var controller. IEEE Transactions on Energy Conversion 1990; 5: 39-45.
[17] Singh, S.; Singh, A.K.; Chanana, S. Operation and control of a hybrid photovoltaic-diesel-fuel cell system connected to micro-grid, IEEE Fifth Power India Conference 2012: 1-6.
[18] Singh, S.; Joshi, H.; Chanana, S.; Verma, R.K. Impact of Superconducting Magnetic Energy Storage on frequency stability of an isolated hybrid power system. International Conference on Computing for Sustainable Global Development 2014:141-145.
[19] Mohd. Hasan Ali, Bin Wu, and Roger A. Dougal. An overview of SMES Applications in Power and Energy Systems. IEEE Transactions on Sustainable Energy 2010; 1: 38-47.
[20] Chen L.Liu, Y. Arsoy A.B., Ribeiro P.F., Steurer M., Iravani M.R. Detailed Modeling of Superconducting Magnetic Energy Storage (SMES) System. IEEE Transactions on Power Delivery 2006; 21:699-709.
[21] M. Mohamed Thameem Ansari, S. Velusami. Dual mode linguistic hedge fuzzy logic controller for an isolated wind-diesel hybrid power system with superconducting energy storage system unit. Energy Conversion and Management 2010; 51:169–181.